Characterizing rheological behavior and fluidization of highly refined furnishes for process optimization

A. JÄSBERG, S. HEISKANEN, J. CECCHINI, T. KIISKINEN, AND A.I. KOPONEN

ABSTRACT: In this work, highly refined softwood bleached kraft pulp (SWBKP) furnishes, referred to here as XFC, were studied from the perspective of fiber suspension handling in processing. The rheology of the furnishes was studied with a rotational rheometer using a non-standard flow geometry to understand the viscosity development at different consistencies and the impact of temperature. For fluidization analysis during pipe flow, two optical methods were implemented; namely, optical coherence tomography (OCT) and high-speed video (HSV) imaging. The OCT was used to determine the small-scale floc structures near the pipe wall where the shear stress is highest, and the HSV imaging was applied for observing flow instabilities and XFC suspension uniformity at the pipe scale. All these issues can be significant in deciding the minimum flow rate required for a process pipe to get sufficient fluidization of XFC suspensions.

Application: The results from this study can be used for studying fluidization conditions or dimensioning process pipes for microfibrillated cellulose (MFC) feeding systems.

The application of microfibrillated cellulose (MFC) in different industrial processes is steadily on the rise, and multiple methods to produce MFC can be found in the literature. The simplest method is extensive refining with a conventional refiner [1]. This method is desirable as it already exists on an industrial scale, but it does not produce pure MFC. The refining produces coarse MFC, which is a mixture of highly fibrillated fibers and fines. With this method, the coarseness or the fines content can be controlled with the amount of refining. However, it is a common tendency for paper and board-making applications to use very coarse MFC, which could be described as highly refined fibers (HRF) like those defined as glue pulp. The main reason for this tendency is likely the effort to reduce refining energy in the production of highly fibrillated materials.

Using MFC as an additive in papermaking has been shown to have many beneficial properties and possible applications. The MFC can be used, for example, to improve the barrier, surface, strength, and optical properties of the produced paper [2-4]. However, using MFC on a paper machine leads to many challenges. Perhaps the biggest challenge is the significant reduction in the dewatering rate caused by increased web sealing [5]. Another challenge is the handling of the MFC furnish during stock preparation and feeding, which is due to the shear thinning and fast reflocculation of the MFC. The furnish must be kept under enough shear to reduce the number of flocs, as a homogeneous suspension is required to achieve, for example, the beneficial strength properties.

In this work, we studied three highly refined furnishes from the perspective of fiber suspension handling in processing. These highly refined softwood bleached kraft pulp (SWBKP) furnishes are referred to as XFC in this study to emphasize that the amount of fibrillation and the number of fines particles in this material is high, but still below that of actual MFC. Three different furnishes were produced by refining and screening, referred to here as XFC1, XFC2, and XFC3. We studied both the rheology and flocculation of these furnishes at different consistencies with a rotational rheometer and pipe flow. The results can be used to evaluate the mixing conditions in tanks, as well as fluidization conditions in process pipes.

MATERIALS AND METHODS

Furnishes

Two softwood bleached kraft pulp (SWBKP) pine furnishes were made at the refining level of 1200 kWh/metric ton (XFC1) and 1400 kWh/metric ton (XFC2). Then, a third furnish (XFC3) was made from XFC2 by screening with a slotted pressure screen (0.15-mm slots, 500 rpm). The refining was done with a Valmet (Espoo, Finland) OptiFiner RF-1 (JC-01) at a consistency of 3% and a flow rate of 15 L/s. Refining curves showing both the drainability (SR) and the water retention value (WRV) are presented in **Fig. 1a**. The drainability was measured with an L&W SR tester (Lorentzen & Wettre; Kista, Sweden) according to ISO 5267-1 "Pulps — Determination of drainability — Part 1: Schopper-Riegler method." For the WRV measurements, a Heraeus Megafuge 8 centrifuge (Thermo Fisher Scientific; Waltham, MA, USA) was utilized, and the measurements were done according to the TAPPI UM 256 Method "Water

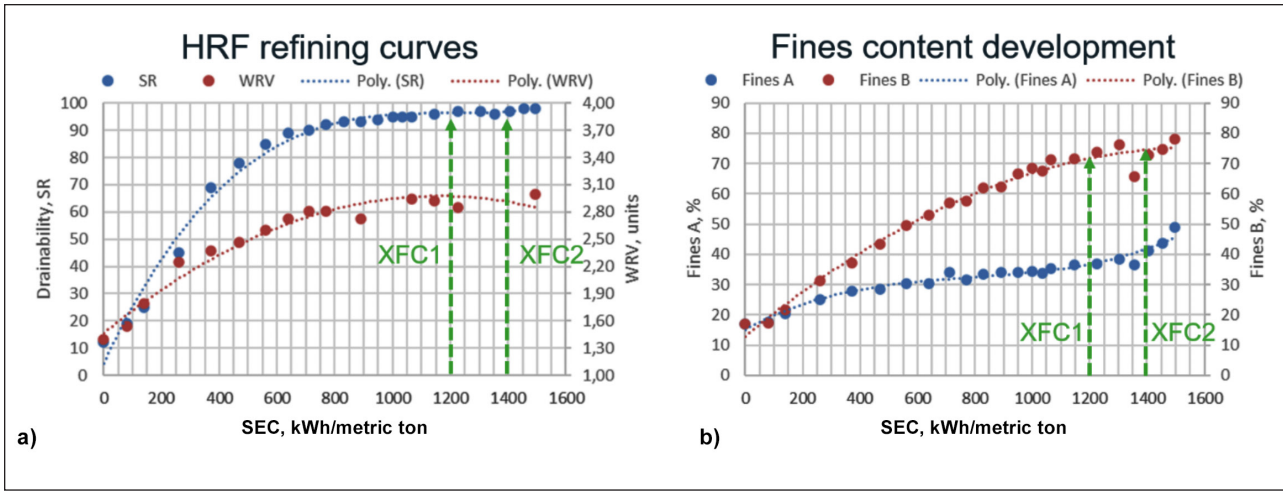

1. a) Refining curves for the highly refined furnishes (HRF), XFC1 and XFC2, showing both the drainability (SR) and the water retention value (WRV) development during the refining; and b) the development of fines content during refining. Fines A are the flake-like fines, and fines B are the fibril-like fines. The arrows show the positions where the test samples were taken (SEC: specific energy consumption).

retention value (WRV)." The furnishes were also characterized with Valmet's fiber image analyzer FS5 to determine the amount of fines in the treated stock (Fig. 1b). The FS5 measures the fractions optically so that fines A is calculated as a percentage of the projection area of particles, and fines B is calculated as a percentage of particle length. Thus, the values are not directly comparable and do not add up to 100%.

Rheology measurements

The rheology studies were done with a TA Instruments (New Castle, DE, USA) rheometer using a nonstandard bucket and vane geometry (**Fig. 2a**). This geometry, a glass bucket with a large gap, was used to eliminate wall slip effects. (Visual inspection confirmed that there was no slip at the bucket wall during measurements; the gap size was thus big enough to eliminate the effect of the gap size on the measurement results.) Moreover, this geometry avoids the possibility that the floc size is comparable with the gap size. The suspension temperature was controlled with a 3D-printed heat bath capsule (Fig. 2b). Heating was performed by recirculating hot water through the capsule.

The rheometer gives the torque (M) as a function of the angular velocity (Ω). If we assume that the material has a yield stress and the shear rate is zero at the bucket wall, the viscosity can be determined from the measurement data using the infinite bucket approximation [6]:

$$\dot{\gamma} = 2M\left(\frac{\partial \Omega}{\partial M}\right) \quad (1)$$

$$\tau = \frac{M}{2\pi h R^2} \quad (2)$$

where $\dot{\gamma}$ and τ are the shear rate and stress, respectively, at the vane tips. The dynamic viscosity μ can then be calculated from Newton's law of viscosity:

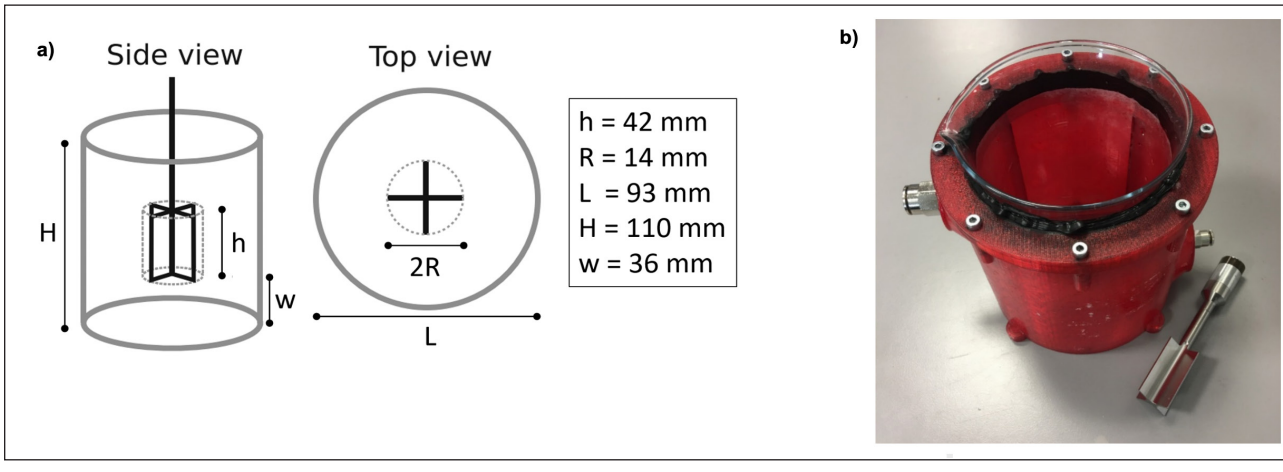

2. a) Schematic of the bucket and vane geometry used for the rheology measurements. b) A 3D-printed heat capsule covering the bucket was used to control the temperature. The TA Instruments vane (type 525.001) used in this study is also shown in the image.

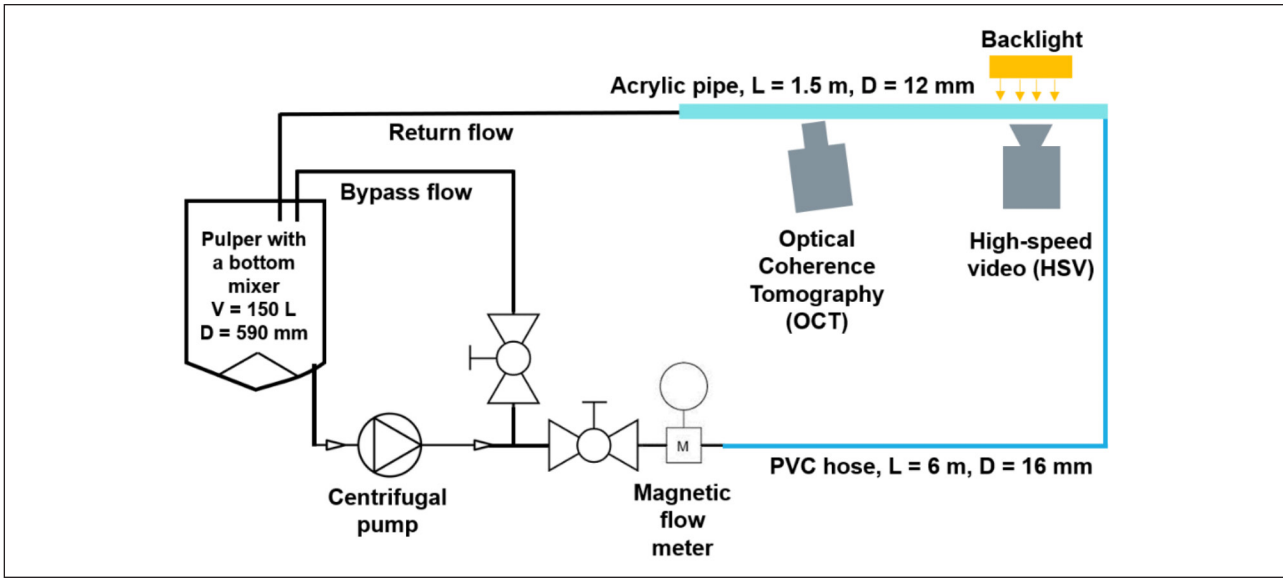

3. Measurement setup for floc size of suspensions during pipe flow.

$$\mu = \frac{\tau}{\dot{\gamma}} \quad (3)$$

The consistency of XFC varied between 0.5% and 2.7%, and the measurements were performed at 21°C and 50°C. The suspension was premixed at 200 rad/s for 2 min. Afterwards, it was allowed to relax for an additional 2 min before the measurements were performed. Premixing is a standard procedure in studying the rheology of dispersions such as MFC. It is performed to ensure sample homogeneity, thereby reducing variability and enhancing result reliability. After premixing, the sample should be allowed to relax for a while to minimize the effect of shear history (thixotropy) on the measurement results. The viscosity measurements were performed with ascending and descending rotational speeds. At each measurement point, the torque was averaged over 2 min. Angular velocity varied between 0.01–30 rad/s (the corresponding shear rates varied between 1 and 150 s^{-1}). A single measurement cycle lasted approximately 60 min. For simplicity, we show here only the descending curves, but viscosity was calculated as the average of both curves. The time dependence of viscosity (thixotropy) was also studied with fixed rotational speeds. Notice that the non-standard bucket we used has a significantly larger volume compared to traditional standard rheometer geometries. The evaporation of water during the measurements had no visible effect on the suspension's surface level in the bucket.

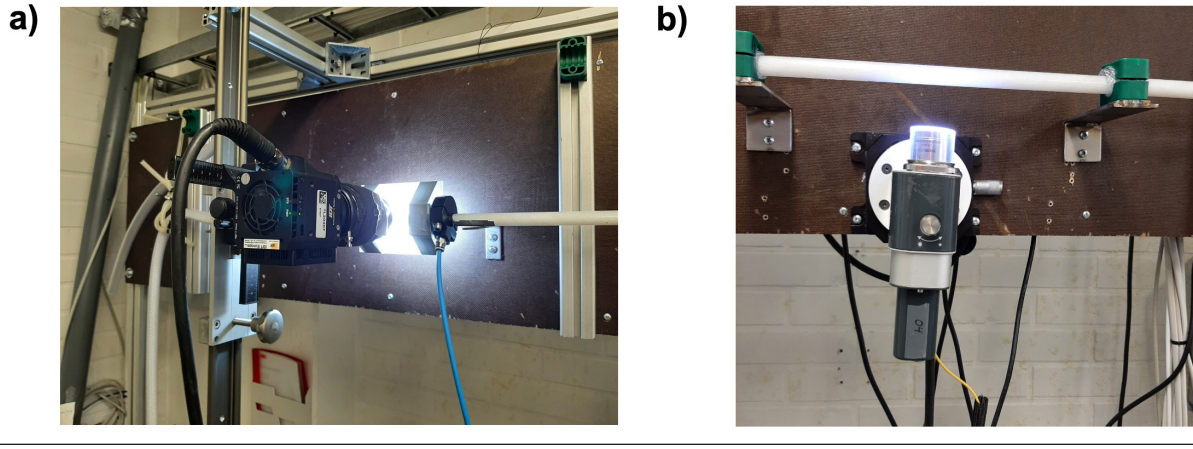

4. a) A high-speed video imaging (HSV) camera was used to obtain large-scale consistency variations (i.e., large-scale floc size) over a 12-mm-long pipe section by using transillumination. b) Optical coherence tomography (OCT) was used to obtain small-scale floc size close to the pipe's inner wall.

Flocculation measurements

Flocculation was measured during pipe flow with the measurement setup shown in **Fig. 3**. We could not efficiently study the flocculation of the XFC3 furnish, because the consistency was too low due to the screening process. We focused the flocculation study on XFC2, as the rheological behavior of XFC1 was very similar. The XFC2 suspension was circulated in the flow loop, and the flocculation measurement was performed in an acrylic pipe having a diameter of 12 mm. The XFC2 consistency varied between 1.0% and 2.3%, and the flow rate varied between 0.2 L/min and 15 L/min. High-speed video (HSV) imaging with a MotionXtra OS3-S3 (Integrated Design Tools; Pasadena, CA, USA) was applied for observing the large-scale consistency variations (i.e., large-scale floc size) at the pipe scale (**Fig. 4a**). The small-scale floc structures near the pipe wall, where the shear stress is highest, were determined using optical coherence tomography (OCT) performed with a Telesto I SD-OCT (Thorlabs; Newton, NJ, USA), as shown in Fig. 4b.

For each trial point, 200—600 HSV images were taken with a pixel resolution of 13 µm. Transillumination was used to improve the image dynamics. To remove the illumination profile, the original images were corrected with a logarithmic average image (**Fig. 5a**). Each image was next binarized with the median of the image (Fig. 5b), and the length-weighted floc size distribution was calculated with the run-length method in the x- and y-directions (Fig. 5c). Finally, the geometric floc size was calculated from the floc size distributions. The image analysis has been explained in detail in [7].

Optical coherence tomography is an optical measurement technique that utilizes low-coherence, near-infrared light for obtaining 1D reflectivity depth profiles (A-scans) of the studied samples [8,9]. The Telesto system's depth pixel resolution is 3.7 µm in water. The scanning rates used were 25 kHz and 91 kHz.

The original OCT images were composed of a long series (of the order of one million) of radial A-scans. The distance between the successive radial scans depends on the OCT imaging frequency and flow velocity, and we calculated only the radial floc size. It is, however, possible to also calculate the axial floc size if the velocity profile close to the wall is also measured with OCT [10,11]. The OCT floc size analysis was performed with the following steps, and the image analysis has been explained in detail in [11]:

- The depth-dependent decay of the OCT signal was first corrected by calculating the average OCT signal as a function of depth and then scaling the pixel values at a given depth with it.
- Noise level of the images was decreased by filtering the images with a median filter (**Fig. 6a**).
- The images were thresholded using Otsu's method (Fig. 6b), which is a widely used technique for image thresholding and segmentation. The goal of Otsu's method is to find an optimal threshold value that separates the pixels in an image into two classes, typically such that the variance within each class is minimized. This threshold value can be used to convert a grayscale image into a binary image.
- Finally, the radial floc size distributions were calculated as run-length distributions (Fig. 6c).

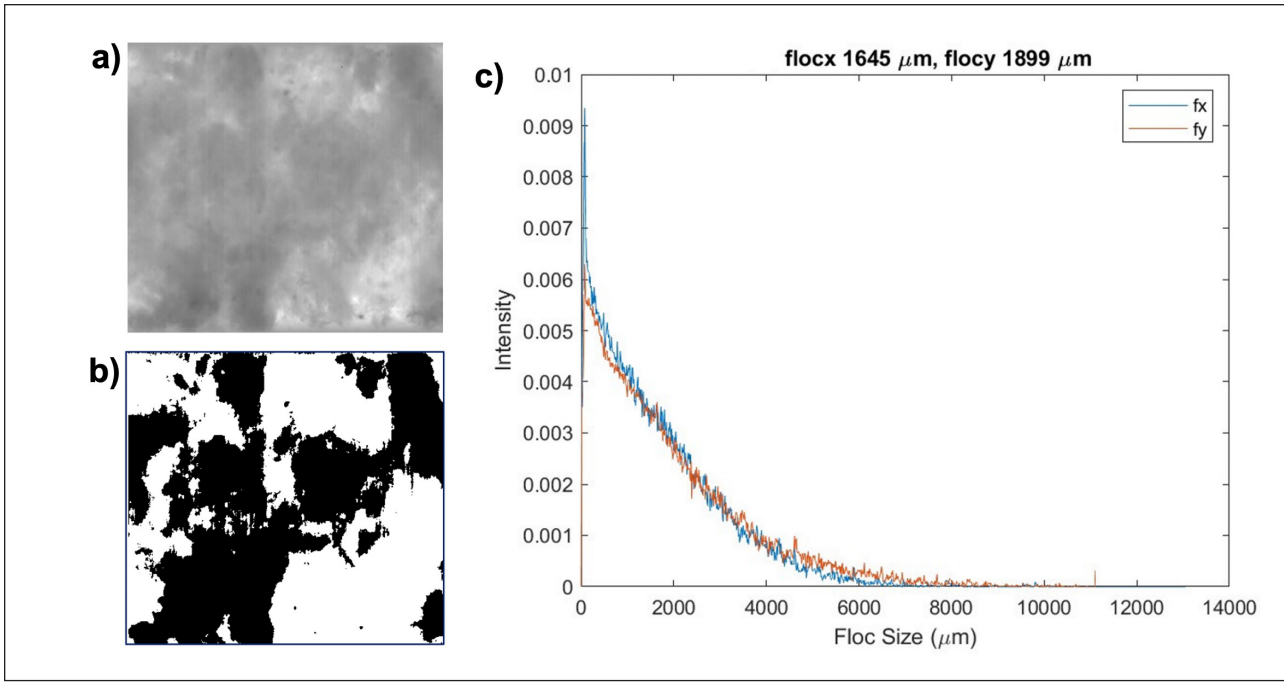

5. a) An HSV image after background illumination correction, with an image height of 12 mm; b) median thresholded binary image; and c) length-weighted floc size distribution in horizontal (x) and vertical (y) directions.

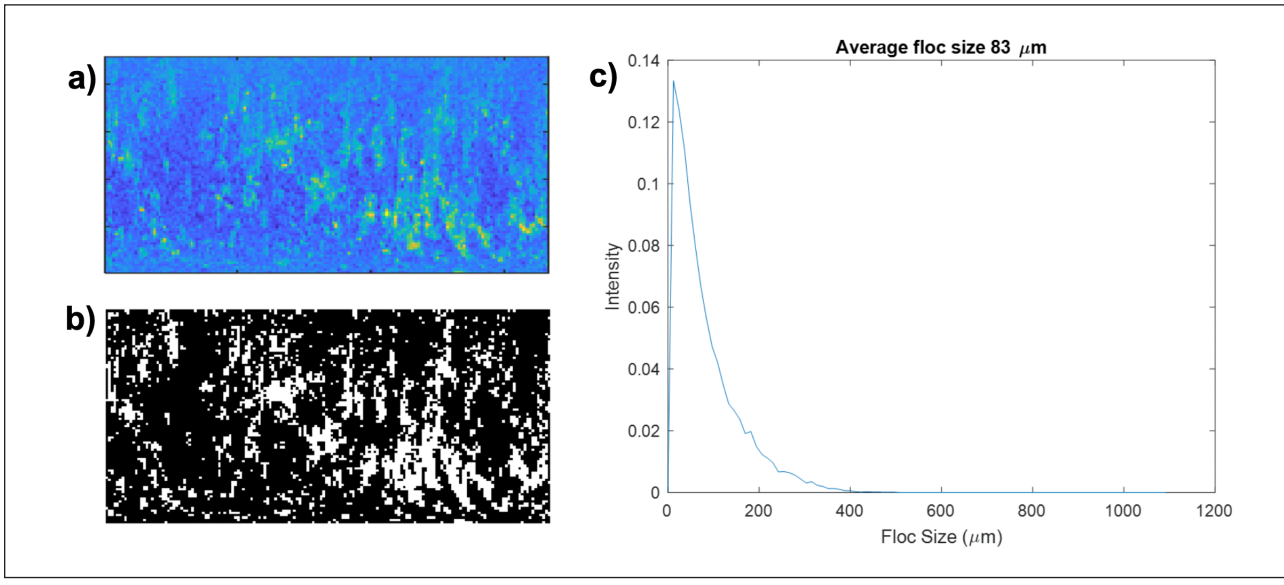

6. a) Small part of the original OCT image after median filtering. The pipe wall is on the bottom. Image height is 1 mm. b) Binarized image obtained with Otsu thresholding. c) Length-weighted radial floc size distribution of the whole OCT image.

RESULTS AND DISCUSSION

Rheological analysis

Figures 7a–b show torque as a function of time for 1% and 2.7% XFC1 for angular velocities of 1 and 10 rad/s. We see from Fig. 7 that, for 1% XFC1, it took approximately 20 min before the torque acting on the vane, measured by the rheometer, was saturated. (This also means that the viscosity of XFC1 was then saturated.) For 2.7% XFC1, saturation took longer, and with 10 rad/s torque, did not saturate during the 30-min measurement. Similar behavior was also seen with other consistencies and furnishes. Torque saturation time was typically 15 to 25 min, and in many cases, torque did not saturate in 30 min. With 1 rad/s, the drop in torque varied between 50% to 75%, and with 10 rad/s, the drop in torque varied between 20% to 40%. Torque saturated more quickly with temperature (T) at 50°C.

In **Fig. 8**, torque is shown as a function of angular velocity for different consistencies of XFC1. We see that torque, and thus viscosity, increased significantly with increasing consistency. Figure 8b compares the torque–angular velocity curves of different XFCs at 0.5% consistency. We see that XFC1 and XFC2 had a similar viscosity, and XFC3 had the highest viscosity.

As discussed previously, the XFC viscosity was calculated from the torque–angular velocity curves with Eqs. 1–3. It was found that, similar to MFCs, XFCs were shear-thinning materials and their viscosity followed the power law with good accuracy:

$$\mu = K\dot{\gamma}^{n-1} \tag{4}$$

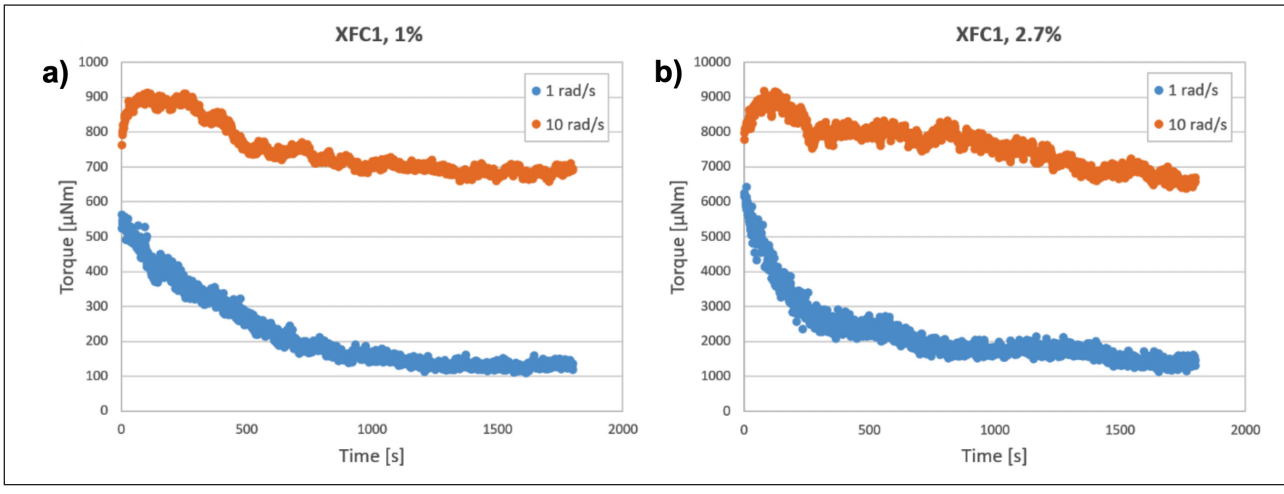

7. Torque as a function of time for: a) 1% XFC1, and b) 2.7% XFC1 with angular velocities of 1 and 10 rad/s. T = 21°C.

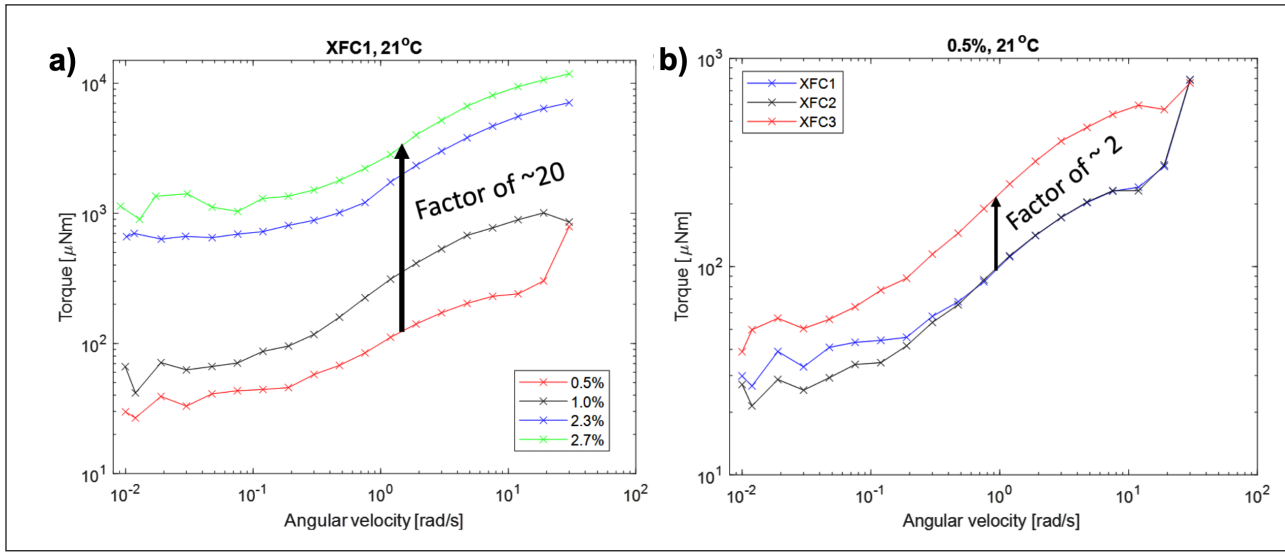

8. a) Torque as a function of angular velocity for different consistencies of XFC1 at T = 21°C; and b) torque as a function of angular velocity for 0.5% XFCs at T = 21°C.

T, °C	21	21	21	21	50	50
C, %	0.5	1	2.3	2.7	1	2.3
K, XFC1	1.06	4.54	28.6	46.3	3.1	17.0
K, XFC2	1.20	5.10	30.9	–	3.1	21.7
K, XFC3	2.83	–	–	–	–	–
n, XFC1	0.31	0.31	0.31	0.31	0.37	0.38
n, XFC2	0.31	0.30	0.31	–	0.37	0.37
n, XFC3	0.30	–	–	–	–	–

I. Values of consistency index (K) and flow index (n) of Eq. 4 for different consistencies and temperatures of XFCs.

where K is the consistency index, and n is the flow index. **Table I** shows the values of K and n for different consistencies and temperatures of XFCs. At T = 21°C, the flow index was around 0.3; this value is similar to that of various grades of MFCs in this consistency region [12].

Figure 9 compares the viscosity of XFCs with the viscosity of various MFC grades reported in the literature. We see that the viscosity of the XFC furnishes was comparable to MFCs, and the relation between viscosity and consistency was approximately a power law, $\mu \propto c^{2.3}$, also for XFCs.

Flocculation analysis

Figures 10a–c show (binarized) HSV images of the 1.9% XFC2 suspension at three flow rates. The large-scale (HSV) floc size of 1.9% XFC2 is shown as a function of flow rate in Fig. 10e. The XFC suspension flow was very heterogeneous at the lowest flow rates below 1 L/min. This led to large spatial consistency variations with big voids, especially next to the pipe wall. The floc size decreased, the homogeneity improved with increasing flow rates, and the

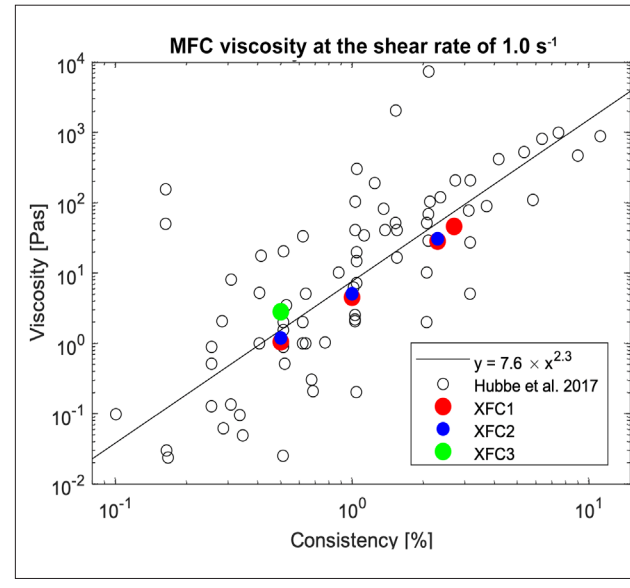

9. Comparison of the viscosity of XFCs with the viscosity of various grades of MFCs at the shear rate of 1.0 s⁻¹ [1].

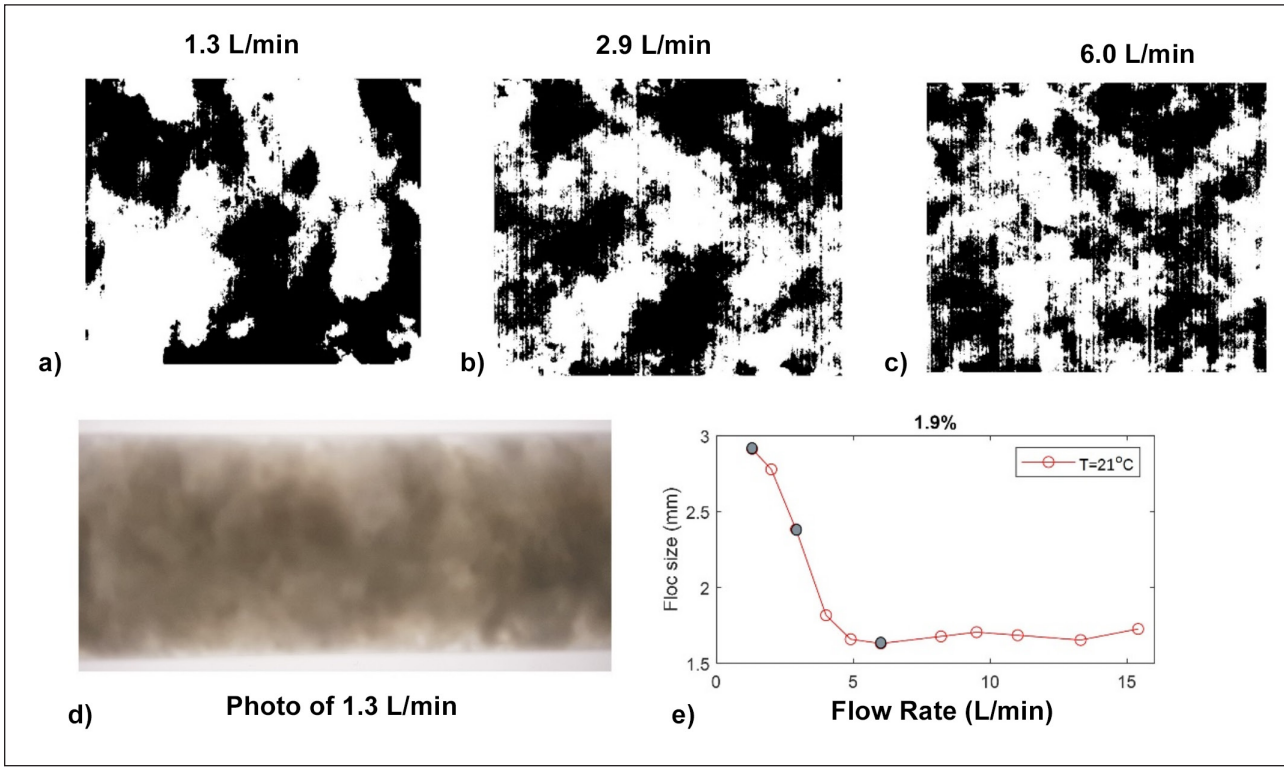

10. Binarized HSV images of the 1.9% XFC2 suspension (T = 21°C) at the flow rates of: a) 1.3 L/min, b) 2.9 L/min, and c) 6.0 L/min. Notice that the vertical lines in the images are an artefact caused by the HSV camera cell. d) Photo of the pipe at the flow rate of 1.3 L/min; and e) large-scale (HSV) floc size at different flow rates. T = 21°C.

	1.0 %	1.5 %	1.9 %	2.3 %
Large-scale floc size	3–4 L/min	5–6 L/min	5–6 L/min	7 L/min
Small-scale floc size	6–8 L/min	6–8 L/min	9–10 L/min	9-10 L/min

II. Flow rate region at which the floc size saturated for different XFC2 consistencies.

large-scale floc size saturated at flow rates that depended on the XFC2 consistency, as shown in **Table II**.

Figures 11 a–c show OCT images of the 1.9% XFC2 suspension at different flow rates. Figure 11d shows the small-scale (OCT) floc size as a function of flow rate. The small-scale floc size saturated at higher flow rates than the large-scale floc size, as shown in Table II. The temperature did not have a noticeable effect on the large-scale or small-scale floc sizes.

CONCLUSIONS

In this work, we analyzed the rheology and flocculation dynamics of highly refined SWBKP furnishes, referred to here as XFC, which share similarities with coarse MFC but retain a substantial fraction of longer fibrils. In our previous investigations concerning flocs using OCT, our focus was on the analysis of pure MFC. On the other hand, previous HSV imaging was used for the analysis of the flocculation of traditional furnish materials. In the present study, we merged these two methodologies. This innovative approach allowed us to simultaneously investigate the dynamics of flocculation of XFC at two different length scales as the flow rate increased. Moreover, to minimize slip effects and ensure accurate monitoring of the true bulk behavior of XFC, we employed a non-standard rheometer geometry with a wider gap size compared to typical standard rheometer configurations.

The rheological behavior of the XFC furnishes was similar to various grades of MFCs, as shown in Fig. 9. The relation between viscosity and consistency followed a similar power law, $\mu \propto c^{2.3}$, as the other MFC furnishes. Of the studied furnishes, the screened XFC3 had the highest viscosity, with XFC1 and XFC2 behaving very similar to each other. This was due to the much shorter fiber length scale of the XFC3. The effect of temperature on the viscosity can be seen in Table I. We observed a 30%–40 % decrease in viscosity when the temperature was increased from 21°C to 50°C. There was also a clear thixotropic effect, as can be

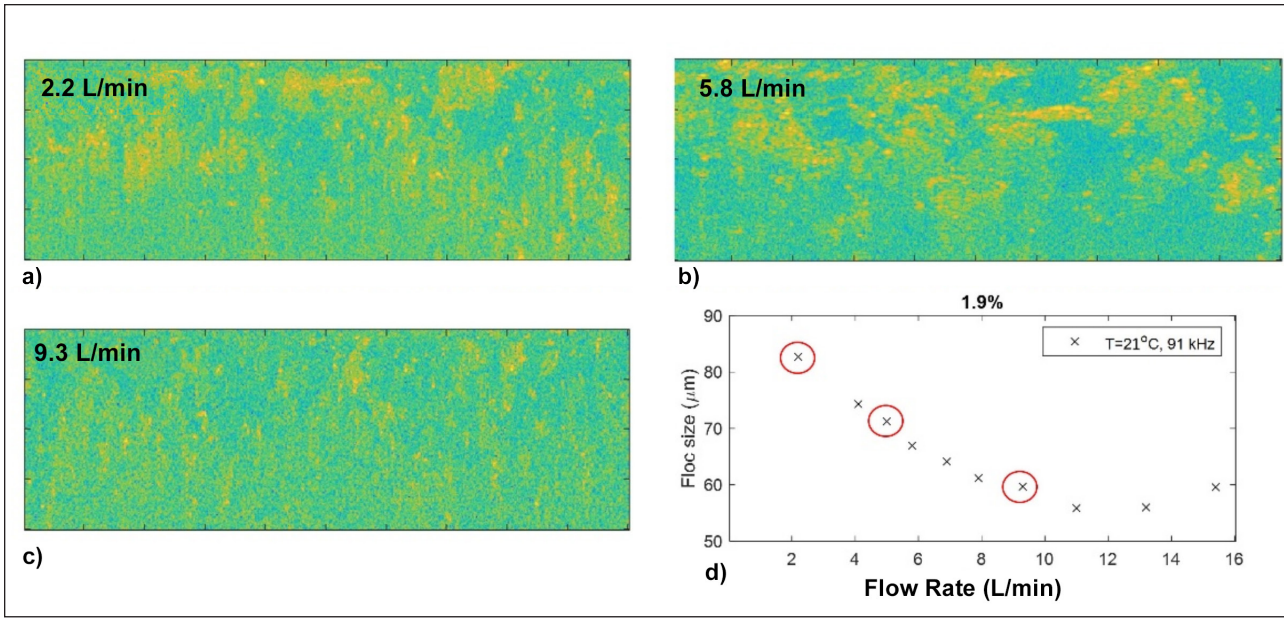

11. The OCT images of the 1.9% XFC2 suspension at the flow rates of: a) 2.2 L/min, b) 5.8 L/min, and c) 9.3 L/min. d) Small-scale (OCT) floc size at different flow rates. T = 21°C.

seen from the constant angular velocity measurements (Fig. 7). The saturation time for the torque varied from 15 to over 30 min. Saturation was generally faster with higher temperature and lower angular velocity. Due to this effect, the shearing history of XFC may significantly alter its rheological behavior during processing. These results can help in evaluating mixing conditions and mixer dimensioning.

The flocculation analysis in pipe flow showed a strong relationship between flow rate and floc size, with both measurement methods, as illustrated in Fig. 10 and Fig. 11. The floc size decreased with increasing flow rate until a saturation point was reached. The large-scale (HSV) and small-scale (OCT) floc size behavior was qualitatively similar, with the small-scale floc size saturating at a slightly higher flow rate. The saturation flow rates increased with consistency, but the temperature had almost no effect on the floc size behavior. The flocculation behavior can be easily scaled by matching apparent shear rates in pipe flow. Thus, these results can be used for studying fluidization conditions or dimensioning process pipes for XFC and MFC feeding systems. **TJ**

LITERATURE CITED

1. Hubbe, M., Tayeb, P., Joyce, M., et al., *BioResources* 12(4): 9556(2017). https://doi.org/10.15376/biores.12.4.Hubbe.
2. Lavoine, N., Desloges, I., Dufresne, A., et al., *Carbohydr. Polym.* 90(2): 735(2012). https://doi.org/10.1016/j.carbpol.2012.05.026.
3. Balea, A., Fuente, E., Concepcion Monte, M., et al., *Molecules* 25(3): 526(2020). https://doi.org/10.3390/molecules25030526.
4. Das, A., Islam, M., Ashaduzzaman, M., et al., *J. Packag. Technol. Res.* 4(3): 253(2020). https://doi.org/10.1007/s41783-020-00097-7.
5. Koponen, A., Cecchini, J., Heiskanen, S., et al., *BioResources* 18(1): 1398(2023). https://doi.org/10.15376/biores.18.1.1398-1419.
6. Coussot, P., *Rheometry of Pastes, Suspensions, and Granular Materials: Applications in Industry and Environment*, John Wiley & Sons, Hoboken, NJ, USA, 2005. https://doi.org/10.1002/0471720577.
7. Kellomäki, M., Karema, H., Kataja, M., et al., "Fiber flocculation measurement in pipe flow by digital image analysis," *TAPPI Int. Pap. Phys. Conf., Proc.*, TAPPI Press, Atlanta, 1999.
8. Popescu, D., Choo-Smith, L.-P., Flueraru, C., et al., *Biophys. Rev.* 3: 155(2011). https://doi.org/10.1007/s12551-011-0054-7.
9. Koponen, A. and Haavisto, S., *KONA Powder Part. J.* 37: 42(2020). https://doi.org/10.14356/kona.2020003.
10. Koponen, A., Lauri, J., Haavisto, S., et al., *Appl. Sci.* 8(5): 755(2018). https://doi.org/10.3390/app8050755.
11. Lauri, J., Haavisto, S., Salmela, J., et al., *Cellulose* 28(6): 3373(2021). https://doi.org/10.1007/s10570-021-03745-6.
12. Koponen, A., *Cellulose* 27(4): 1879(2020). https://doi.org/10.1007/s10570-019-02908-w.

ABOUT THIS PAPER

Cite this article as:
Jäsberg, A., Heiskanen, S., Cecchini, J., et al., *TAPPI J.* 23(4): 200(2024). https://doi.org/10.32964/TJ23.4.200

DOI: https://doi.org/10.32964/TJ23.4.200

ISSN: 0734-1415

Publisher: TAPPI Press

About this journal

ABOUT THE AUTHORS

We chose this topic because there is a need to elucidate the true rheological and fluidization responses of highly refined fibers (referred to here as XFC), which are frequently employed in various industrial applications under the name of microfibrillated cellulose (MFC). Different applications of XFC require a comprehensive understanding of the necessary agitation conditions for fluidization at various consistencies, including revolutions per minute, effective shear rate, and mixing time. In contrast with true MFC, there is a scarcity of published data regarding the rheological and flocculation behavior of XFC.

The most difficult aspect of this study was developing such measurement methods that consider the distinctive properties of XFC, especially the remarkably broad fiber/fibril size distribution of XFC.

The primary practical discovery in this study concerned the flow rate/shear rate regimes in which XFC achieves effective fluidization. Our most surprising observation was the similarity in the rheological behavior of XFC when compared to MFC.

From this study, mills gain an understanding of the relationship between the appropriate combination of agitation times and fluidization regimes for a specific XFC application. The next step is to expand this study to include other XFC furnishes and determine their optimal fluidization conditions for use in papermaking applications.

Jäsberg is senior scientist, Kiiskinen is research scientist, and Koponen is principal scientist at VTT Technical Research Centre of Finland in Jyväskylä, Finland. Heiskanen is development engineer and Cecchini is senior development manager at Valmet Technologies in Jyväskylä, Finland. Email Koponen at Antti.Koponen@vtt.fi.

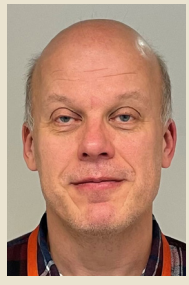
Jäsberg

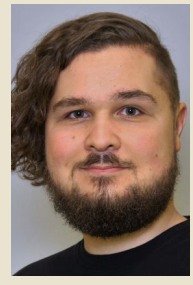
Heiskanen


Cecchini


Kiiskinen


Koponen